Eur Biophys J (2013) 42:103–118
DOI 10.1007/s00249-013-0887-z

ORIGINAL PAPER

EBSA
Biophysics in Europe

Folding and stability of outer membrane protein A (OmpA) from *Escherichia coli* in an amphipathic polymer, amphipol A8-35

Cosmin L. Pocanschi · Jean-Luc Popot · Jörg H. Kleinschmidt

Received: 21 November 2012 / Accepted: 2 January 2013 / Published online: 1 February 2013

Abstract Amphipols are a class of amphipathic polymers designed to maintain membrane proteins in aqueous solutions in the absence of detergents. Denatured β-barrel membrane proteins, like outer membrane proteins OmpA from *Escherichia coli* and FomA from *Fusobacterium nucleatum*, can be folded by dilution of the denaturant urea in the presence of amphipol A8-35. Here, the folding kinetics and stability of OmpA in A8-35 have been investigated. Folding is well described by two parallel first-order processes, whose half-times, $\sim$5 and $\sim$70 min, respectively, are independent of A8-35 concentration. The faster process contributed $\sim$55–64 % to OmpA folding. Folding into A8-35 was faster than into dioleoylphosphatidylcholine bilayers and complete at ratios as low as $\sim$0.17 g/g A8-35/OmpA, corresponding to $\sim$1–2 A8-35 molecules per OmpA. Activation energies were determined from the temperature dependence of folding kinetics, monitored both by electrophoresis, which reports on the formation of stable OmpA tertiary structure, and by fluorescence spectroscopy, which reflects changes in the environment of tryptophan side chains. The two methods yielded consistent estimates, namely $\sim$5–9 kJ/mol for the fast process and $\sim$29–37 kJ/mol for the slow one, which is lower than is observed for OmpA folding into dioleoylphosphatidylcholine bilayers. Folding and unfolding titrations with urea demonstrated that OmpA folding into A8-35 is reversible and that amphipol-refolded OmpA is thermodynamically stable at room temperature. Comparison of activation energies for folding and unfolding in A8-35 versus detergent indicates that stabilization of A8-35-trapped OmpA against denaturation by urea is a kinetic, not a thermodynamic phenomenon.

Keywords Membrane protein folding · Amphipols · Kinetics · Thermodynamic stability · Outer membrane protein · A8-35

Abbreviations

A8-35	A specific type of amphipol
APol	Amphipol
Borate	Sodium tetraborate-10-hydrate
diC_{10}PC	1,2-Dicapryl-*sn*-glycero-3-phosphocholine
diC_{12}PC	1,2-Dilauroyl-*sn*-glycero-3-phosphocholine
diC_{12}PG	1,2-Dilauroyl-*sn*-glycero-3-phosphoglycerol
DOPC	1,2-Dioleoyl-*sn*-glycero-3-phosphocholine
EDTA	Ethylenediaminetetraacetic acid
FomA	Major outer membrane protein from *Fusobacterium nucleatum*
KTSE	Kinetics of tertiary structure formation determined by electrophoresis
LDAO	*N*-Lauryl-*N*,*N*-dimethylammonium-*N*-oxide

Special issue: Structure, function, folding and assembly of membrane proteins—insight from Biophysics.

C. L. Pocanschi · J. H. Kleinschmidt
Fachbereich Biologie, Universität Konstanz,
78457 Konstanz, Germany

C. L. Pocanschi
Tanz Centre for Research in Neurodegenerative Diseases,
University of Toronto, Toronto, ON M5S 3H2, Canada

J.-L. Popot
UMR 7099, Centre National de la Recherche Scientifique
and Université Paris-7, Institut de Biologie Physico-Chimique,
13 rue Pierre et Marie Curie, 75005 Paris, France

J. H. Kleinschmidt (✉)
Abteilung Biophysik, Institut für Biologie, Universität Kassel,
Heinrich-Plett-Straße 40, 34132 Kassel, Germany
e-mail: jhk@uni-kassel.de

MOMP	Major outer membrane protein from *Chlamydia trachomatis*
OMP	Outer membrane protein
OmpA	Outer membrane protein A from *Escherichia coli*
PAGE	Polyacrylamide gel electrophoresis
SDS	Sodium dodecyl sulfate
TMP	Transmembrane protein
Tris	Tris-(hydroxymethyl)-aminomethane

Introduction

Membrane protein folding and insertion has attracted much interest over the past three decades, because the principles and mechanisms by which the different types of transmembrane proteins (TMPs) fold are not well understood. It is important to understand the basic concepts of membrane protein folding in relation to amino acid sequence, the role of chaperones, folding catalysts and the protein import machinery in membranes. In addition, the development of methods to fold integral membrane proteins to their active form is of significant technological importance. Pharmacologically important membrane proteins, e.g., G-protein-coupled receptors, often need to be folded to their active form when expressed heterologously (Banères et al. 2011). Tools to refold membrane proteins may be important also for engineered mutants or chimeric membrane proteins. Until recently, investigations into the principles and mechanisms of TMP folding have been performed mostly either with detergent or lipid/detergent micelles or with preformed lipid bilayers (Buchanan 1999; Kiefer 2003; Kleinschmidt 2006; Kleinschmidt et al. 2011; Popot and Engelman 2000).

Recent work has demonstrated great promise for the use of a class of amphipathic polymers called amphipols [APols; for a recent review, see Popot et al. (2011)]. TMPs of the two structural classes, their transmembrane domains featuring either an α-helical bundle or a β-barrel, have been successfully folded to their functional three-dimensional structure using various APols (Banères et al. 2011; Bazzacco et al. 2012; Dahmane et al. 2009, 2011, 2013; Leney et al. 2012; Pocanschi et al. 2006b). APols are short polymers comprising both hydrophilic groups and hydrophobic chains, which can substitute for detergents to provide a milder, stabilizing environment to solubilized TMPs (Popot 2010; Popot et al. 2003, 2011; Sanders et al. 2004; Tribet et al. 1996). The best characterized and most widely used APol to date, known as A8-35, is obtained by derivatizing polyacrylic acid with octylamine and isopropylamine, leaving ~35 % of the carboxylic groups free (Gohon et al. 2006; Tribet et al. 1996). In aqueous solutions, A8-35 molecules, whose number-averaged molecular mass, $\langle M_n \rangle$, is ~4.3 kDa (see footnote 1), assemble into small micelle-like particles of ~40 kDa at pH 6.8–9.2 in the presence of ~100 mM salt (Gohon et al. 2004, 2006; Perlmutter et al. 2011). APols form stable, water-soluble complexes with TMPs by adsorbing onto their hydrophobic transmembrane surface (Althoff et al. 2011; Catoire et al. 2009, 2010). Most TMPs are stable for a longer time and at higher temperature as complexes with APols than they are in detergent solutions [reviewed in Popot (2010), Popot et al. (2011)]. The underlying mechanisms are complex and appear to involve at least three factors: the poor ability of APols to compete with stabilizing protein/protein and protein/lipid interactions, which accounts for their weak detergency; reduction of the hydrophobic sink due to the excess of surfactant, which is made possible by the very low critical association concentration of APols (Giusti et al. 2012); and, possibly, damping of conformational excursions, due to the viscosity of the polymer backbone [for a discussion, see Popot et al. (2011)]. While the slowing down of denaturation kinetics is a very general observation, no study has been reported yet of the thermodynamic stability of APol-trapped TMPs. The kinetics of folding of an α-helical TMP, bacteriorhodopsin, upon dilution of a denatured form from an SDS solution into APol A8-35 has been reported recently, but not analyzed in details (Dahmane et al. 2013).

Successful folding in APol A8-35 of two β-barrel TMPs, OmpA from *Escherichia coli* and FomA from *Fusobacterium nucleatum*, was first described by Pocanschi et al. (2006b). This study demonstrated that A8-35 is not only stabilizing membrane proteins in solutions, but also provides an environment capable of inducing the formation of β-barrels with a hydrophobic surface and a polar lumen. Both FomA and OmpA were kept water-soluble by A8-35 and both transferred spontaneously from the TMP/A8-35 complex to preformed lipid bilayers, leading to the formation of ion channels with their typical conductance (Pocanschi et al. 2006b). No data on the kinetics of folding of OmpA nor on its stability in A8-35 have been reported to date. This information is nevertheless important, because it could lead to new insights into principles of folding and stability of β-barrel TMPs. OmpA has been a favorite model in studies of the folding of bacterial outer membrane proteins (OMPs), because it is relatively small and a monomer. The first 171 residues of OmpA fold into an 8-stranded β-barrel domain (Pautsch and Schulz 1998; Vogel and Jähnig 1986) that spans the outer membrane of *E. coli*, while the last 154 residues form a soluble periplasmic domain. Whole-length OmpA has been folded in detergent micelles (Kleinschmidt et al. 1999b; Surrey and Jähnig 1992), in lipids (Kleinschmidt

and Tamm 2002; Patel et al. 2009; Surrey and Jähnig 1992), and in APol A8-35 (Pocanschi et al. 2006b). The isolated β-barrel (tOmpA) has been folded in detergent micelles (Pautsch and Schulz 1998; Surrey and Jähnig 1992) and in sulfonated APols (Dahmane et al. 2011). The β-barrel of OmpA has been shown to fold into lipid bilayers by a concerted mechanism, in which the association of neighboring β-strands is coupled to penetration of the β-barrel into the hydrophobic region of the membrane (Kleinschmidt et al. 1999a, 2011; Kleinschmidt and Tamm 2002). More recently, OmpA was used as an engineering platform to monitor receptor-ligand interactions, by replacing its outer loops by those of the human Y1 G protein-coupled receptor (Walser et al. 2011, 2012). These chimeras were still able to fold from their urea-unfolded forms after dilution into detergent solution, demonstrating that folding of the eight-stranded β-barrel does not depend on the sequence of these loops.

In the present study, we investigated whether A8-35 leads to faster folding of OmpA in comparison to lipid membranes, the native environment of membrane proteins. We analyzed the folding kinetics and determined the A8-35/OmpA ratio required for quantitative refolding of OmpA. From the temperature dependence of the kinetics of folding into A8-35, we estimated the corresponding activation energies. Last, we investigated the thermodynamic stability of OmpA trapped in A8-35 (Pocanschi et al. 2006b) and compared it to its stability in lipid bilayers and detergent micelles.

Materials and methods

Materials

Amphipol A8-35 was synthesized and purified by F. Giusti (UMR 7099) as described previously (Gohon et al. 2004, 2006). OmpA was purified from *E. coli* strain P400 as described previously (Surrey and Jähnig 1992). OmpA concentrations of stock solutions were determined using the method of Lowry et al. (1951). LDAO was from Fluka (Buchs, Switzerland). All other chemicals were purchased from standard sources such as Sigma (Steinheim, Germany) and were of analytical grade.

SDS–polyacrylamide gel electrophoresis

SDS–polyacrylamide gel electrophoresis (SDS-PAGE) was performed as described previously (Bulieris et al. 2003) using the method of Laemmli (1970) with the modifications described by Weber and Osborne (1964), but without heat denaturation of the samples.

Determination of fraction of folded OmpA by SDS-PAGE

This assay is based on the different electrophoretic mobilities of folded (apparent molecular mass 30 kDa) and unfolded OmpA (apparent molecular mass 35 kDa) in sodium dodecyl sulfate polyacrylamide gel electrophoresis (SDS-PAGE), when samples are not heat-denatured before electrophoresis. The 30 kDa form has been shown by Raman, Fourier-transform-infrared, and circular dichroism spectroscopy (Dornmair et al. 1990; Kleinschmidt et al. 1999b; Rodionova et al. 1995; Sugawara et al. 1996; Surrey and Jähnig 1992, 1995; Vogel and Jähnig 1986), by phage inactivation assays (Schweizer et al. 1978), and by single channel conductivity measurements (Arora et al. 2000) to correspond to the native structure of OmpA. The fraction of folded OmpA is determined by densitometry of the stained polyacrylamide gels as described previously (Bulieris et al. 2003; Kleinschmidt 2003; Kleinschmidt and Tamm 1996, 2002).

Kinetics of tertiary structure formation by electrophoresis (KTSE)

Folding reactions were initiated by rapidly diluting 10 µL urea-denatured OmpA into 180 µL of Borax/NaOH buffer (10 mM, pH 10.0, with 2 mM EDTA) containing A8-35. The final concentrations of OmpA were 7.2 µM in experiments to determine the kinetics of folding as a function of A8-35 concentration and 15 µM in experiments to determine the kinetics of folding as a function of temperature, respectively. Samples of the reaction mixture were taken at different times after the initiation of folding, and an equal volume of 0.125 M Tris buffer, pH 6.8, containing 4 % SDS, 20 % glycerol, 10 % 2-mercaptoethanol and 0.01 % Coomassie Brilliant Blue R-250 was added. SDS binds to both folded and unfolded OmpA and inhibits further folding (Kleinschmidt 2003; Kleinschmidt and Tamm 1996; Surrey and Jähnig 1995). To obtain the time course of OmpA folding, the fraction of folded OmpA was determined for each of the samples taken at the different times.

Trypsin digestion experiments

Since folded and inserted OmpA is digested only partially, leaving the transmembrane β-barrel domain and a small part of the periplasmic domain intact, inaccessibility of the OmpA transmembrane domain to trypsin digestion was tested also after OmpA folding into A8-35, as described previously (Surrey and Jähnig 1992). In short: samples containing 0.4 mg/mL OmpA were incubated with trypsin at 0.04 mg/mL at 37 °C for 2 h. Digestion was stopped by

addition of 0.04 mg/mL soybean trypsin inhibitor. An equal volume of 0.125 M Tris buffer, pH 6.8, containing 4 % SDS, 20 % glycerol, 10 % 2-mercaptoethanol and 0.01 % Coomassie Blue was added and samples were analyzed by SDS-PAGE (12 % acrylamide). 4 μg OmpA were loaded per lane.

Folding kinetics monitored by fluorescence spectroscopy

Fluorescence kinetics were started by rapidly mixing 14 μL denatured OmpA with 986 μL of borate buffer (10 mM, pH 10, with 2 mM EDTA) containing A8-35 at a mass ratio of 8 g/g A8-35/OmpA (that is ~65 A8-35 molecules per OmpA[1]), unless stated otherwise. The final OmpA concentration was 1.25 μM. To monitor OmpA folding, spectra were recorded immediately after addition of OmpA and at various time points up to 480 min after mixing. Samples were slowly stirred between measurements. All fluorescence intensities of OmpA at 330 nm were divided by the fluorescence intensity of OmpA in 8 M urea at the same temperature to correct for the temperature dependence of the fluorescence of OmpA.

Analysis of folding kinetics

To examine the kinetics of OmpA folding into amphipol A8-35, a model (Kleinschmidt and Tamm 2002; Patel et al. 2009) assuming two parallel kinetic processes was fitted to the data as described previously for KTSE experiments [see Patel et al. (2009) for details].

In the fits, the initial concentrations (at $t = 0$) of the unfolded protein $[P_U]_0$, and of amphipol $[A]_0$ that were used in the experiment were known invariable parameters. The rate constants of the first (k_1) and the second kinetic process (k_2), the relative contributions A_f and $1 - A_f$ of each of the kinetic processes, and the fraction of OmpA that has folded in the end of the folding reaction, R, were the four fit parameters. In two parallel folding processes, described by first order kinetics, the mole fraction X_F of folded OmpA at time t, can be written as (Patel et al. 2009):

$$X_F(t) = R\{1 - [A_f \exp(-k_f t) + (1 - A_f)\exp(-k_s t)]\} \quad (1)$$

This equation was fitted to the kinetic data reported in this study. For fluorescence kinetics, fluorescence signals were normalized by the initial fluorescence intensity in aqueous urea-solution to obtain $FR(t) = F(t)/F_0$. For fits to $FR(t)$ versus t, Eq. 1 becomes:

$$FR(t) = 1 + (f_R - 1) \cdot X_F(t)$$

where f_R is the ratio of the fluorescence signals (f_{FP}/f_{AQP}) of folded and unfolded forms of OmpA, respectively.

Binding/folding of A8-35 to unfolded OmpA monitored by gel electrophoresis

Folding reactions were initiated by rapidly diluting 10 μL of urea-denatured OmpA into 180 μL of Borax/NaOH buffer (10 mM, pH 10.0, with 2 mM EDTA) containing A8-35. The final concentrations of OmpA were 7.2 μM in all experiments at A8-35/OmpA ranging from 0.5 to 16 g/g. SDS-PAGE and densitometric analysis of folded and unfolded forms of OmpA were used to determine the fraction of folded OmpA. Functions describing OmpA folding into A8-35 were fitted to the experimental data assuming that OmpA reacts with n A8-35 molecules with indistinguishable affinity.

In this case, the average concentration of bound A8-35, $[B]$, is given by a simple mass action law that can be rewritten to (van Holde et al. 2006):

$$[B]/[\mathrm{OMP_T}] = nK_{ass}[F]/(1 + K_{ass}[F]), \quad (2)$$

where n is the number of A8-35 molecules in OmpA/A8-35 complexes, K_{ass} the association constant, $[\mathrm{OMP_T}]$ the total concentration of the outer membrane protein, and $[F]$ the concentration of the A8-35 available for complex formation with OmpA. Substitution of $[F]$, with the total A8-35 concentration, $[L_0] = [B] + [F]$, and some rearrangements lead to (Qu et al. 2007):

$$[B] = {}^1\!/_2\Big\{K_{ass}^{-1} + [L_0] + n[\mathrm{OMP_T}] - \Big(\big(K_{ass}^{-1} + [L_0] + n[\mathrm{OMP_T}]\big)^2 - 4n[\mathrm{OMP_T}][L_0]\Big)^{1/2}\Big\}. \quad (3)$$

Equilibrium unfolding monitored by fluorescence spectroscopy

To estimate and compare the thermodynamic stabilities ($\Delta G°$) of OmpA in either LDAO micelles or in A8-35, we performed equilibrium unfolding experiments and recorded fluorescence spectra of OmpA at different concentrations of the denaturant. For equilibrium unfolding/folding experiments, equilibration was monitored starting from

[1] The molecular mass of A8-35 was previously reported to be 8–10 kDa, depending on the source of polyacrylic acid. This estimate was based on size exclusion chromatography analyses in aqueous solvent using polyethyleneglycol polymers as standards of molecular mass (Gohon et al. 2006; Tribet et al. 1996). A recent reexamination of this issue, using absolute calibration, has yielded the revised number-averaged mass $\langle M_n \rangle \approx 4.3$ kDa (Giusti and Rieger, personal communication). This value will be used in the present article. This revision does not affect any of the conclusions that have been published thus far regarding the mass, composition and properties of A8-35 particles and TMP/A8-35 complexes.

either unfolded or folded forms in two different sets of experiments. In each of these sets, equilibration was monitored at selected urea concentrations until no further changes in fluorescence spectra were observed.

To monitor equilibration starting from the unfolded form, 1.4 µL of unfolded OmpA (31.4 mg/mL) in 10 M urea were mixed with 998.6 µL of an A8-35 solution (0.35 mg/mL) in borate buffer (10 mM pH 10, 2 mM EDTA) containing urea at different concentrations, ranging from 0 to 10 M. The A8-35/OmpA ratio was 8 g/g and the final OmpA concentration was 1.3 µM in a total volume of 1 mL.

To monitor equilibration starting from the folded state, 26 µL folded OmpA (1.6 g/L) in A8-35 at a ratio A8-35/OmpA of 8 g/g were mixed with 974 µL borate buffer (10 mM pH 10, 2 mM EDTA) containing different urea concentrations from 0 to 10 M urea.

All samples were incubated at 40 °C until equilibration was reached. Similarly, these procedures were applied for folding-unfolding reactions of OmpA in LDAO micelles at a molar LDAO/OmpA ratio of 800, which is above the CMC (He et al. 2012).

Fluorescence spectra were recorded as described previously (Bulieris et al. 2003) on a Spex Fluorolog-3 spectrofluorometer with double monochromators in the excitation and emission pathways. The excitation wavelength was 290 nm, and the bandwidths of the excitation monochromators were 2 nm. The bandwidths of the emission monochromators were 3.7 nm. The integration time was 0.05 s, and an increment of 0.5 nm was used to scan spectra in the range of 300–380 nm. Three scans were averaged for each sample.

Determination of the free energy of unfolding

For a two state equilibrium between the folded (F) and unfolded (U) states of a protein, the free energy of the unfolding transition (ΔG°) is given by:

$$\Delta G^\circ_{F\rightarrow U} = -RT\ln(K) = -RT\ln\left(\frac{1-X_F}{X_F}\right), \quad (4)$$

where X_F is the concentration of the folded protein, T the temperature in Kelvin, R the universal gas constant and K the equilibrium constant. The free energy of unfolding depends linearly on the concentration of the denaturant urea in the transition region, and can be obtained by extrapolation to 0 M urea [see e.g. Pace (1990), Pace et al. (1998)]:

$$\Delta G^\circ_{F\rightarrow U} = \Delta G^\circ_{F\rightarrow U}(H_2O) - m\cdot c(\text{urea}). \quad (5)$$

Fluorescence emission spectra of OmpA (f_λ) are characterized by the intensity-weighted average fluorescence emission maximum $\langle\lambda_F\rangle$:

$$\langle\lambda_F\rangle = \frac{\sum f_\lambda\cdot\lambda}{\sum f_\lambda}. \quad (6)$$

$\langle\lambda_F\rangle$ can be used to relate the fluorescence of a mixture of folded and unfolded protein to the equilibrium constant K. It can be shown that for of a mixture of folded and unfolded states, the intensity-weighted average fluorescence emission maximum of the mixture $\langle\lambda_M\rangle$, relates to that of the folded, $\langle\lambda_F\rangle$, and unfolded $\langle\lambda_U\rangle$ forms of a protein (Hong and Tamm 2004; Roumestand et al. 2001; Royer et al. 1993):

$$\langle\lambda_M\rangle = \frac{\langle\lambda_F\rangle + \frac{1}{Q_R}K\langle\lambda_U\rangle}{\left(1+\frac{1}{Q_R}K\right)} \quad \text{with} \quad Q_R = \frac{\sum_\lambda f_\lambda(S_F)}{\sum_\lambda f_\lambda(S_U)}. \quad (7)$$

$f_\lambda(S_F)$ and $f_\lambda(S_U)$ are the fluorescence intensities of the spectra of the folded and unfolded forms as a function of the wavelength. Equations (4), (5), and (7) can be combined to

$$\langle\lambda_M\rangle = \frac{\left(\langle\lambda_{F,0}\rangle + m_F\cdot c_D\right) + \left(\langle\lambda_{U,0}\rangle + m_U\cdot c_D\right)\frac{1}{Q_R}e^{-\frac{\Delta G^\circ(H_2O)}{RT}-m\frac{c_D}{RT}}}{\left(1+\frac{1}{Q_R}e^{-\frac{\Delta G^\circ(H_2O)}{RT}-m\frac{c_D}{RT}}\right)}. \quad (8)$$

Equation 8 was used to fit unfolding titrations of OmpA with urea.

Results

OmpA isolated in unfolded form in 8 M urea is known to fold, at neutral or basic pH, into micelles of neutral or zwitterionic detergents (Kleinschmidt et al. 1999b; Surrey and Jähnig 1992) as well as into lipid bilayers. Refolding has been shown for bilayers composed either of a range of pure phosphatidylcholine species with fatty acyl chains of various lengths (Kleinschmidt and Tamm 2002) or of mixtures of lipids with various head-groups (Bulieris et al. 2003; Patel et al. 2009). We have previously shown that OmpA also folds when urea is strongly diluted in the presence of A8-35. Evidence for folding in A8-35 was obtained from CD spectroscopy, SDS-PAGE, protease digestion, and the formation of characteristic ion channels upon insertion into black lipid bilayers (Pocanschi et al. 2006b).

OmpA folds rapidly and to high yields into A8-35

To investigate the stoichiometry of OmpA interactions with A8-35 and the basic mechanism of OmpA folding into A8-35, kinetic studies were performed as a function of the concentration of A8-35 (Fig. 1). In a first set of experiments, unfolded OmpA (0.252 g/L, that is 7.2 µM) in 8 M urea was mixed with A8-35 at mass ratios of 0.5, 1, 2, 6, 8,

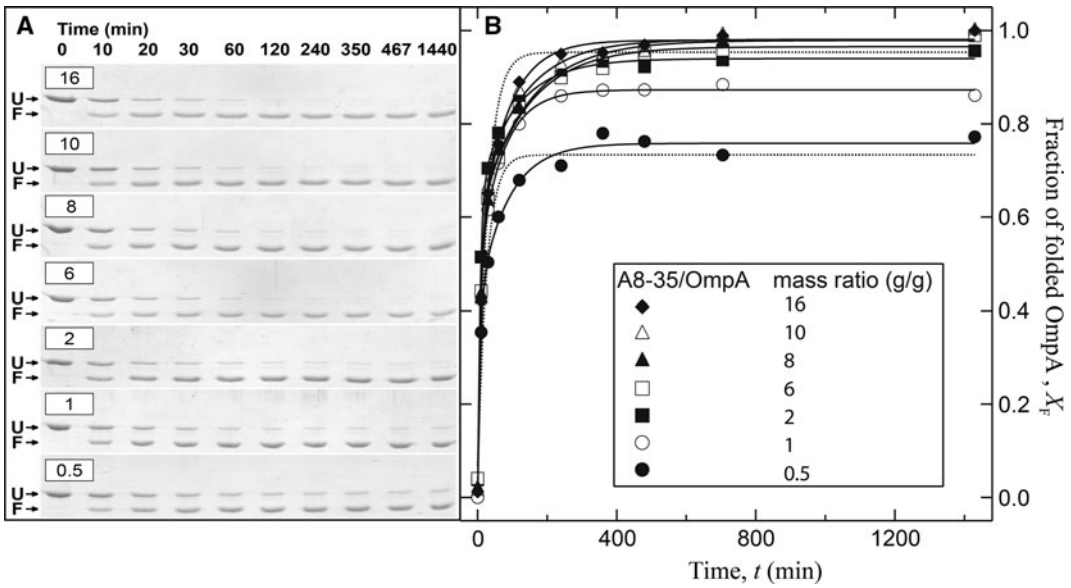

Fig. 1 Kinetics of insertion and folding of OmpA into A8-35 at different concentrations of A8-35. **a** SDS–polyacrylamide gels demonstrating the formation of folded OmpA (*F*) as a function of increasing incubation time after initiating folding of urea-unfolded OmpA (*U*) by dilution of the denaturant in the presence of A8-35. Unfolded OmpA migrated at 35 kDa, folded OmpA at 30 kDa. The concentration of OmpA was 7.2 μM in all gels. The concentration of A8-35 ranged from 0.126 to 4.032 g/L, so that the mass ratios APol/OmpA were 0.5, 1, 2, 6, 8, 10, and 16 g/g (from *bottom* to *top*). Taking an average molecular mass for A8-35 of 4.3 kDa (see footnote 1), this would correspond to molar A8-35/OmpA ratios of 4.1, 8.1, 16.3, 48.8, 65.1, 81.4 and 130.3, respectively. Only sections of each gel containing unfolded and folded OmpA monomers are shown. **b** Fraction of folded OmpA, determined by densitometry of the gels shown in **a**, plotted as a function of time. All folding reactions were performed at 40 °C in 10 mM borate buffer, pH 10.0, containing 2 mM EDTA. Equation (1) (*solid lines*) and a single exponential function, $X(t) = A \exp(-k \cdot t) + B$, with *A*, *B*, and *k* as three free fit parameters (*dotted lines*), were fitted to the data

10, and 16 g A8-35 per g OmpA, under concurrent strong dilution of the urea. For each mass ratio, the time course of folding was determined by SDS-PAGE (see "Materials and methods") (Fig. 1a). Folded OmpA (*F*) migrates at an apparent M_r of 30 kDa, unfolded OmpA (*U*) at 35 kDa. Even at the relatively low mass ratio of 0.5 g/g A8-35/OmpA, high folding yields were obtained within 1 h. Intermediate folding forms have been reported for OmpA folding into DOPC lipid bilayers at 30 °C by SDS-PAGE (Kleinschmidt and Tamm 1996) and by fluorescence quenching (Kleinschmidt et al. 1999a, 2011; Kleinschmidt and Tamm 1999). They were not observed in the present experiments, either because they did not accumulate under our experimental conditions or because they unfolded again in the presence of SDS. SDS-PAGE therefore reports only on the rate of formation of the final, SDS-stable folded form. If the folding reaction involves several sequential steps, what is being monitored here is the final one. This last step can comprise kinetically distinguishable parallel processes.

For quantitative analysis, the fraction of folded OmpA, $X_F = F / (F + U)$, was determined by densitometric analysis of the bands and plotted as a function of time (Fig. 1b). The time course of OmpA folding could not be well fitted by simple single-process kinetics, i.e. a single-exponential time course (Fig. 1b, dotted lines). Rather, it indicated the presence of two distinguishable parallel pathways. This is similar to previous observations for the folding kinetics of outer membrane proteins into lipid bilayers (Patel et al. 2009; Pocanschi et al. 2006a). As discussed below, parallel phases may result from different coexisting protonation states of OmpA. The charges of OmpA side-chains may indeed affect the interactions of OmpA with negatively charged A8-35.

Equation 1 (see "Materials and methods") describes the folding kinetics for two parallel first-order or pseudo-first-order processes and has been a good model for the analysis of OmpA folding into lipid bilayers of different composition based on electrophoretic mobility shifts (Patel et al. 2009). The two rate constants, the relative contribution of the faster kinetic process, and the fraction of OmpA folded at the end of the reaction were the parameters obtained from fits of Eq. 1 to the experimental data and are shown in Table 1. On average, the faster process contributed ~65 % to OmpA folding with a half time of ~5 min, whereas the slower process had a half time of ~70 min. Neither rate constant depended much on the concentration of A8-35, which ranged from 0.126 to 4.03 g/L (i.e., ~13 to ~420 μM, see footnote 1), while the OmpA concentration was 7.2 μM (0.252 g/L) in all experiments. The

Table 1 Rate constants of OmpA folding into A8-35 at different concentrations

T^a (°C)	$[P]^b$(μM)	$[A]^c$ (g/L)	$[A]/[P]$ g/g	k_f^d (min^{-1})	k_s^e (min^{-1})	A_f^f	R^g
Fits to kinetics composed of two first-order processes							
40	7.2	0.126	0.5	0.143 ± 0.038	0.011 ± 0.003	0.55 ± 0.07	0.76 ± 0.02
40	7.2	0.252	1	0.155 ± 0.014	0.014 ± 0.001	0.56 ± 0.03	0.87 ± 0.00
40	7.2	0.504	2	0.137 ± 0.018	0.009 ± 0.002	0.70 ± 0.04	0.94 ± 0.01
40	7.2	1.512	6	0.118 ± 0.020	0.008 ± 0.001	0.62 ± 0.05	0.97 ± 0.01
40	7.2	2.016	8	0.111 ± 0.014	0.007 ± 0.001	0.61 ± 0.03	0.98 ± 0.01
40	7.2	2.520	10	0.097 ± 0.012	0.008 ± 0.002	0.64 ± 0.04	0.98 ± 0.01
40	7.2	4.032	16	0.123 ± 0.020	0.013 ± 0.002	0.53 ± 0.05	0.98 ± 0.01

Equation (1) was fitted to the data shown in Fig. 1b, which assumes two parallel first-order processes. The rate constants of the two kinetic processes, the relative contribution of the fast process, and the final folding yield were free-fit parameters (see "Materials and methods")

[a] Temperature, [b] concentration of OmpA (~0.252 g/L), [c] concentration of A8-35 in g/L, [d] rate constant of the fast process, [e] rate constant of the slow process, [f] relative contribution of the fast process, [g] final fraction of folded OmpA

independence of the rate constants on the concentration of APol indicates that the two folding processes are indeed of first order. In pseudo-first-order or higher-order reactions, the rate constants usually depend on the concentration of the reaction partner, even if it is present in large excess.

Estimation of the stoichiometry of folding of OmpA into A8-35

To estimate the stoichiometry of folding of OmpA into A8-35, we plotted the yields of folded OmpA obtained at different A8-35 concentrations (Fig. 1) as a function of the molar A8-35/OmpA ratio (Fig. 2). These data indicate that folding of OmpA is complete at a mass ratio of ~2 g/g (~16 mol/mol). However, the data also show that ~80 % of OmpA folded already at the much lower mass ratio of 0.5 g/g (4 mol/mol). Equilibrium unfolding experiments (see below) indicated that, thermodynamically, unfolding and folding are described by a two-state equilibrium. To obtain a crude estimate on the stoichiometry and free energy of folding of OmpA in A8-35, we applied a simplified model in which OmpA reacts with n A8-35 molecules, from an oligomeric A8-35 particle (Gohon et al. 2006; Zoonens et al. 2007), with indistinguishable affinity, and assumed that this reaction would be reversible as well at the low urea concentration of ~420 mM used here. A simple mass action law, Eq. 3 (see "Materials and methods"), was fitted to the data of Fig. 2. This yielded an average stoichiometry of $n \approx (1.4 \pm 3.9)$ mol/mol for the interaction of A8-35 with OmpA, which corresponds to a mass ratio of 0.172 g/g A8-35/OmpA at pH 10 and at 420 mM urea (errors of the fitting parameters were estimated based on a confidence interval of 99 %). This model yields only an estimate of the stoichiometry. It neither allows conclusions regarding the size of reaction

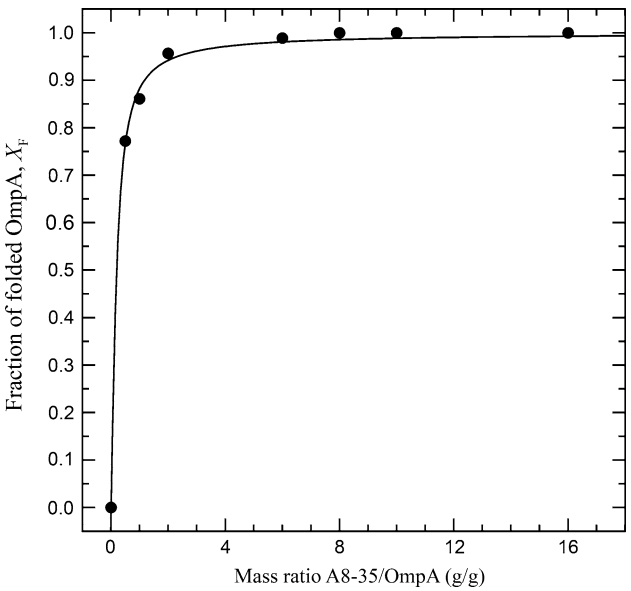

Fig. 2 Dependence of the final yield of OmpA folding on A8-35 concentration. Fractions of folded OmpA were determined after 1 day of incubation at different concentrations of A8-35 by densitometry of the gels shown in Fig. 1a. Taking an average molecular mass for A8-35 of 4.3 kDa, the mass ratios on the x axis would correspond to molar A8-35/OmpA ratios of 4.1, 8.1, 16.3, 48.8, 65.1, 81.4 and 130.3. The data were analyzed by fitting a mass action law for the reaction of unfolded OmpA with A8-35 (Eq. 3). Experiments were performed at 40 °C, pH 10, and 420 mM urea in 10 mM borate buffer. The total concentration of OmpA (7.2 μM) was an invariable parameter in these fits. A crude estimate of the stoichiometry was obtained from these fits, namely 1.4 ± 3.9 A8-35 molecules per OmpA, with an association constant $K_{ass} \approx 4.3 \pm 3.6\ \mu M^{-1}$ (see text for details)

partners nor regarding the total mass of the complexes formed. The association/folding constant calculated from these fit is $K_{ass} \approx (4.3 \pm 3.6)\ \mu M^{-1}$ ($K_{diss} \approx$ 230 nM), which would correspond to a free energy

$\Delta G^{\circ} \approx -32.2 \pm 4.7$ kJ/mol (-7.7 kcal/mol) for folding at pH 10 in the presence of 420 mM urea. Despite the electrostatic repulsion between OmpA and A8-35 at pH 10, in the absence of salt, this affinity is quite high. The affinity (and probably the stoichiometry as well) are likely higher under more usual conditions, that is, in the absence of urea and at pH 8 with ~100 mM salt.

Temperature-dependence of OmpA folding into A8-35 investigated by SDS-PAGE

To investigate the activation energies of the two processes of folding into A8-35, experiments were performed at temperatures ranging from 10 to 50 °C. Folding kinetics were first investigated with SDS-PAGE [Kinetics of Tertiary Structure formation by Electrophoresis, KTSE (Kleinschmidt 2003, 2006), see "Materials and methods"]. The gels shown in Fig. 3a indicate that kinetics were slower and yields of folded OmpA smaller at lower temperatures. However, in contrast to OmpA folding into lipid bilayers of dioleoyl phosphatidylcholine (DOPC) (Kleinschmidt and Tamm 1996), formation of the folded form was still observed at 20 °C or below, and even reached 50 % after 7 h at 10 °C.

To determine the rate constants of the folding kinetics, the fraction of folded OmpA was determined by densitometry and plotted as a function of time at each temperature (Fig. 3b). Again, the data were correctly fitted by two parallel first-order processes (Eq. 1). The corresponding rate constants, relative contributions of the fast and slow processes, and folding yields are shown in Table 2a. The rate constant of the faster process showed little dependence on the temperature, while that of the slower process increased about 6–7-fold from 10 to 50 °C. Folding yields increased with temperature from ~68 % at 10 °C to ~95 % at 30 °C and above, which tallies with the higher relative contribution of the fast folding process and with the increased rate constant of the slower process at higher temperature. Activation energies, calculated from Arrhenius plots of the temperature dependency of the rate constants (Fig. 4) were $\sim 5.9 \pm 4.1$ kJ/mol (~1.4 kcal/mol) for the fast process and $\sim 36.5 \pm 9.6$ kJ/mol (~8.7 kcal/mol) for the slow process. The activation energies for the slower process have a larger standard deviation, arising from the slow folding rates for this process in particular at the low temperatures and from the lower fraction of OmpA that folds via this pathway at the higher temperatures.

Temperature dependence of OmpA folding kinetics as determined by fluorescence spectroscopy

Whereas kinetics obtained from KTSE experiments report on the final stage of the folding of OmpA, the initial folding steps and binding of unfolded OmpA to A8-35 may be resolved by fluorescence spectroscopy, as demonstrated in previous studies on the folding of OmpA into lipid bilayers (Kleinschmidt and Tamm 1996, 2002; Surrey and Jähnig 1992, 1995). Intrinsic fluorescence spectra are sensitive to the hydrophobicity of the local environment of the five tryptophan residues of OmpA, which changes upon folding of OmpA and/or its interaction with the hydrophobic regions of A8-35. All five fluorescent tryptophans of OmpA are located in its transmembrane domain and their replacement by phenylalanine largely eliminates the fluorescence emission when OmpA is excited at 290 nm (Kleinschmidt et al. 1999a). Solution NMR data have

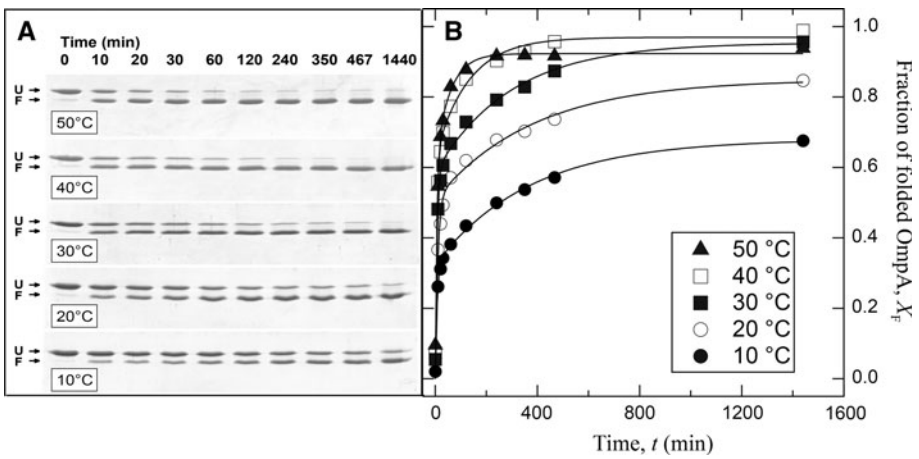

Fig. 3 Temperature dependence of the kinetics of insertion and folding of OmpA into A8-35 as determined by KTSE. **a** Each SDS–polyacrylamide gel shows the formation of the folded form of OmpA with increasing incubation time. Experiments were performed at 10, 20, 30, 40, and 50 °C. The concentration of OmpA was 15 μM and the A8-35/OmpA ratio 8 g/g in all experiments. **b** The gels of **a** were analyzed by densitometry and the fraction of folded OmpA plotted as a function of time. The data were fitted to Eq. 1, described in the "Materials and methods" section (*solid lines*)

Table 2 Rate constants for folding of OmpA into A8-35 at different temperatures and contribution of the fast process, A_f

(A) OmpA insertion and folding into A8-35 (KTSE)

T^a (°C)	$[P]^b$(μM)	$[A]^c$ (g/L)	$[A]/[P]$ g/g	k_f^d (min^{-1})	k_s^e (min^{-1})	A_f^f	R^g
10	15	4.2	8	0.141 ± 0.020	0.0027 ± 0.0003	0.47 ± 0.02	0.68 ± 0.01
20	15	4.2	8	0.107 ± 0.022	0.0026 ± 0.0008	0.60 ± 0.04	0.85 ± 0.04
30	15	4.2	8	0.152 ± 0.027	0.0034 ± 0.0008	0.62 ± 0.03	0.95 ± 0.03
40	15	4.2	8	0.178 ± 0.048	0.0077 ± 0.0029	0.65 ± 0.05	0.97 ± 0.03
50	15	4.2	8	0.162 ± 0.070	0.018 ± 0.011	0.67 ± 0.14	0.92 ± 0.02

(B) OmpA insertion and folding into A8-35 (fluorescence)

T^a (°C)	$[P]^b$(μM)	$[A]^c$ (g/L)	$[A]/[P]$ g/g	k_{ff}^d (min^{-1})	k_{fs}^e (min^{-1})	A_f^f	R^g
5	1.25	0.35	8	0.12 ± 0.11	0.011 ± 0.005	0.56 ± 0.131	0.68
10	1.25	0.35	8	0.082 ± 0.034	0.007 ± 0.003	0.65 ± 0.09	0.68
20	1.25	0.35	8	0.092 ± 0.05	0.009 ± 0.004	0.64 ± 0.12	0.85
30	1.25	0.35	8	0.096 ± 0.062	0.012 ± 0.006	0.62 ± 0.17	0.95
40	1.25	0.35	8	0.102 ± 0.056	0.013 ± 0.006	0.66 ± 0.14	0.97
50	1.25	0.35	8	0.14 ± 0.58	0.04 ± 0.11	0.7 ± 1.9	0.92

[a] Temperature, [b] concentration of OmpA in μM (this is 0.525 g/L in the KTSE experiments of Table 2A and 0.04375 g/L in the fluorescence experiments of Table 2B), [c] concentration of A8-35, [d] rate constant of the fast process, [e] rate constant of the slow process, [f] relative contribution of the fast process, [g] folding yield as obtained from Table 2A, used as an invariable parameter in the fits to the fluorescence kinetics

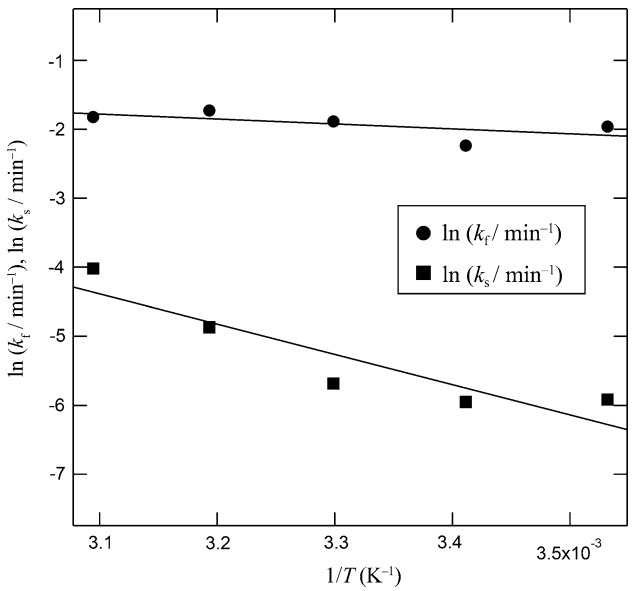

Fig. 4 Arrhenius plot for determining activation energies for the folding of OmpA into A8-35. The logarithms of the rate constants, determined from the double exponential fits shown in Fig. 3b, were plotted against the reciprocal absolute temperature. The activation energies for each of the two folding processes were obtained from linear fits

shown that, in native OmpX/A8-35 complexes, aromatic side chains of the protein interact with alkyl chains of the polymer (Catoire et al. 2009).

Fluorescence spectra of OmpA were therefore recorded at different times after dilution of the denaturant in the presence of A8-35. The kinetics were analyzed by plotting the increase in the fluorescence intensity at 330 nm as a function of time, followed at temperatures ranging from 5 to 50 °C (Fig. 5a). Fluorescence kinetics showed the largest fluorescence changes at 50 °C and much smaller relative changes at 5 °C (Fig. 5a). The calculated rate constants exhibited Arrhenius-type temperature dependences. Activation energies were determined to be 8.8 ± 2.3 kJ/mol for the fast process and 28.9 ± 8.1 kJ/mol for the slower process, respectively. Within the error margins, these energies compare well with those determined by the KTSE method. Since the fluorescence changes report on changes in the hydrophobicity of the environment of the fluorescent amino acids of the protein, especially tryptophan, the comparison suggests that folding and interaction/insertion of OmpA into A8-35 are coupled, as described previously for OmpA folding into lipid bilayers (Kleinschmidt 2006; Kleinschmidt et al. 1999a, 2011; Kleinschmidt and Tamm 2002). However, in comparison, the activation energy for OmpA folding into DOPC bilayers (small unilamellar vesicles, SUVs) was determined previously to be 46 kJ/mol (Kleinschmidt and Tamm 1996). There is therefore a much lower energy barrier to OmpA folding into A8-35 than into DOPC bilayers.

In this context, it is interesting to note that A8-35 is a negatively charged APol with a considerable number of free carboxyl groups. It has been determined that, already at pH 6.8, all carboxylates are deprotonated (Gohon et al. 2004). This corresponds to ~105–110 charges per

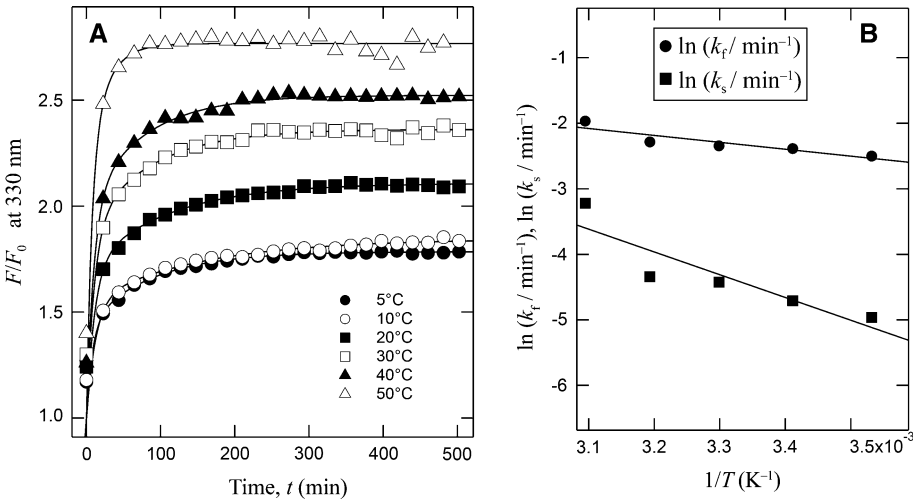

Fig. 5 Temperature dependence of the kinetics of interaction of OmpA with A8-35 as determined by fluorescence measurements. **a** Time-course of A8-35-induced changes of the intrinsic tryptophan fluorescence of OmpA after urea dilution in the presence of A8-35. The concentration of OmpA was 1.25 μM and the mass ratio A8-35/OmpA 8 g/g. Fluorescence kinetics were fitted to Eq. 1 as described in the "Materials and methods" section. **b** Arrhenius plots of the logarithm of the rate constants, determined from the double exponential fits shown in **a**, versus the reciprocal temperatures at which the reactions were performed. The activation energies for each of the two folding processes were determined from linear fits

~40 kDa particle, or an average of ~11–12 charges per molecule. The barrel assembly machinery (BAM) complex of the *E. coli* outer membrane is comprised of five proteins (BamA to BamE). The essential components are BamA and BamD, both of which bear a strong negative surface potential and partially surface-exposed hydrophobic groves. It is possible that the surface of A8-35 particles, with its high density of negative charges and partial exposure of the hydrophobic core (Perlmutter et al. 2011), be in part physically similar to that of the extramembrane domains of the BAM proteins.

Equilibrium unfolding

To compare the effects of A8-35 and LDAO on the stability of OmpA, equilibrium unfolding titrations were performed with OmpA refolded either in LDAO (Fig. 6a) or in A8-35 (Fig. 6b). Unfolding was induced by again increasing the concentration of urea. The progress of unfolding was monitored by fluorescence spectroscopy as a function of the concentration of urea and of the incubation time, the latter ranging from 3 to 52 days. Intensity-weighted average fluorescence emission maxima $\langle\lambda_M\rangle$ of fluorescence spectra were calculated and plotted as a function of urea concentration. The progress of unfolding of OmpA at each urea concentration and incubation time is shown in Fig. 6 (filled symbols). Refolding experiments were performed in parallel (Fig. 6, open symbols), in which urea-denatured OmpA was diluted into solutions of either LDAO (Fig. 6a) or A8-35 (Fig. 6b) and let to refold at various residual concentrations of urea. The concentrations of OmpA, LDAO or A8-35 were the same as in the unfolding experiments. Samples were again incubated for up to 52 days.

When the equilibrium was reached, the unfolding and refolding titration curves superimposed. This was observed after 25 days of incubation in LDAO micelles (Fig. 6a, filled bow tie, open bow tie) (at 0.229 g/L LDAO, that is 5.24 g LDAO per g OmpA), but only after 52 days of incubation in A8-35 (Fig. 6b, filled bow tie, open bow tie) (at 0.35 g/L A8-35, that is 8 g A8-35 per g OmpA). For unfolding titration curves, the midpoint remained near 8 M urea for about 17 days and shifted to ~6 M urea after 25 days. In contrast, the midpoint for folding was observed at ~6 M urea already after 3 days. For folding into A8-35, the midpoint was at ~2 M urea. Therefore, folding OmpA in A8-35 required a stronger dilution of urea than folding in LDAO. Unfolding of OmpA from the A8-35-trapped folded form was characterized by a midpoint of unfolding near 7 M urea when samples were incubated for 3 days (filled circle, open circle). However, 3 days of incubation were insufficient for complete equilibration, which took ~52 days and was characterized by midpoints at ~2 M urea, corresponding to the folding mid-point observed 3 days after mixing.

To determine the free energy of unfolding of OmpA in A8-35 and in LDAO, Eq. (8) was fitted to the folding and unfolding titrations shown in Fig. 6. Equation 8 assumes that the dependence of the Gibbs free energy, $\Delta G°$, on the urea concentration is linear in the titration region, where folded and unfolded forms of a protein coexist. This has been shown for wide range of soluble proteins (Pace and

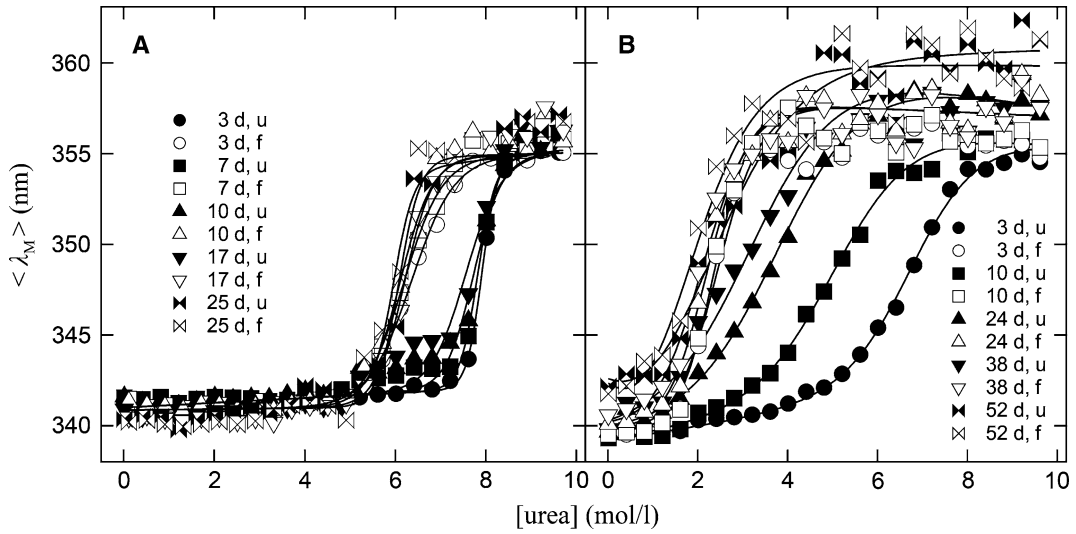

Fig. 6 Unfolding (*solid symbols*) and refolding (*open symbols*) titrations of OmpA in LDAO (**a**) and in A8-35 (**b**) in the presence of various concentrations of urea, determined by fluorescence spectroscopy. Samples of OmpA in LDAO were incubated for 3 (*filled circle*, *open circle*), 7 (*filled square*, *open square*), 10 (*filled triangle*, *open triangle*), 17 (*inverted filled triangle*, *inverted open triangle*), and 25 (*filled bow tie*, *open bow tie*) days (**a**) and samples of OmpA in A8-35 for 3 (*filled circle*, *open circle*), 10 (*filled square*, *open square*), 24 (*filled triangle*, *open triangle*), 38 (*inverted filled triangle*, *inverted open triangle*), 52 (*filled bow tie*, *open bow tie*) days (**b**) at 40 °C. The concentration of OmpA was 1.25 μM in all experiments. The A8-35/OmpA ratio was 8 g/g (∼65 mol/mol) and the LDAO/OmpA ratio 5.24 g/g (800 mol/mol). Experiments were performed in borate buffer (10 mM, pH 10, 2 mM EDTA). Equation (8) was fitted to the experimental data (*solid lines*)

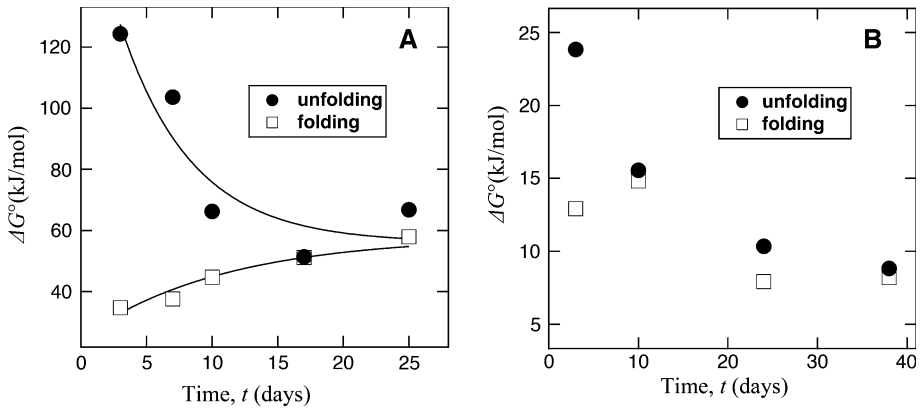

Fig. 7 Energies of unfolding calculated by fitting the data of Fig. 6 to Eq. (8). Equilibrium was reached after 25 days for LDAO **a** and after 52 days for A8-35 **b**, respectively. At equilibrium, free energies of unfolding were ∼60 kJ/mol for OmpA in LDAO solution and ∼8 kJ/mol for A8-35-trapped OmpA

Shaw 2000) and also for membrane proteins (Hong and Tamm 2004). Fits of Eq. 8 to the experimental data are typically performed to calculate the free energy of folding/unfolding extrapolated to 0 M urea, which determines the stability of the protein. Only an apparent Gibbs free energy, ΔG°_{app}, is obtained from these fits unless titrations for folding and unfolding superimpose and show complete reversibility. Figure 7 shows the calculated ΔG°_{app} (that is the extrapolated free energy at 0 M urea) for all titrations performed in LDAO (Fig. 7a) or in A8-35 (Fig. 7b) as a function of the incubation time. The apparent Gibbs free energies for unfolding and for folding approached each other with time, indicating equilibration. Equilibration took 18–25 days in LDAO (Fig. 7a) and 30–40 days in A8-35 (Fig. 7b). The free energy of stabilization of OmpA in the absence of urea was calculated to be $\Delta G^{\circ}_{LDAO} \approx 60$ kJ/mol (14.3 kcal/mol) in LDAO and $\Delta G^{\circ}_{A8\text{-}35} \approx 8$ kJ/mol (1.9 kcal/mol) in A8-35 (in borate buffer, 10 mM pH 10.0, containing 2 mM EDTA). The stability of OmpA in LDAO compares well to that recently reported for the stability of OmpA in octylmaltoside, $\Delta G^{\circ}_{octylmaltoside} \approx 65.2$ kJ/mol (15.6 kcal/mol) (Andersen et al. 2012). It indicates that OmpA is more stable in detergents than in lipid bilayers of small unilamellar vesicles. Indeed, a free energy of stabilization $\Delta G^{\circ} \approx 14.2$ kJ/mol (3.4 kcal/mol) has been reported for OmpA in lipid bilayers composed of palmitoyl-oleoyl-phosphatidylcholine and palmitoyl-oleoyl-phosphatidylglycerol (sonicated, small unilamellar vesicles, SUVs, 10 mM phospholipid, in 10 mM glycine buffer, pH 10.0, containing 2 mM EDTA) (Hong and Tamm 2004).

Discussion

Parallel pathways of OmpA folding into A8-35

A8-35 is a highly efficient tool for folding OmpA. Only small amounts of APol are needed. Folding is faster and simpler than into lipid bilayers of small unilamellar vesicles of DOPC (Kleinschmidt and Tamm 1996) and comparable to folding into large unilamellar vesicles of dicapryl phosphatidylcholine (*di*C_{10}PC) (Kleinschmidt and Tamm 2002), both of which require vesicle preparation procedures. In comparison to detergents like LDAO, A8-35 has a very low critical aggregation concentration (Giusti et al. 2012) and can still be used under very dilute refolding conditions. Those would require much larger amounts of detergents, given that OmpA does not fold into a monomeric detergent (Kleinschmidt et al. 1999b). A8-35 has proven to be a tool of choice for proteins that are hard to fold, as is the case of G-protein-coupled receptors (Dahmane et al. 2009).

Independent of the analytical method used, namely SDS-PAGE versus fluorescence spectroscopy, OmpA appeared to fold following two parallel first-order processes. Neither process depended on the concentration of A8-35 (which ranged from ~0.126 to ~4.03 g/L, corresponding to ~30 to ~940 μM), consistent with their first-order kinetics. As described previously for the folding of OmpA from a chaperone-bound state into bilayers of lipids with various headgroup compositions (Patel et al. 2009), as well as for the folding of another outer membrane protein, FomA from *F. nucleatum* (Pocanschi et al. 2006a), into bilayers of *di*C_{10}PC or DOPC, no intermediate forms are detectable on the gels. Intermediate forms likely exist, but they are not stable enough to survive exposure to SDS (some outer membrane proteins, like Tsx or YaeT from *E. coli* are not even stable enough in their native form to display two bands in this electrophoresis protocol). The electrophoretic analysis therefore only reports on the appearance of natively folded OmpA, which, in the present experiments, results from two parallel processes (Fig. 1b).

The reason for the existence of parallel processes might be that, near pH 10, lysine or tyrosine side-chains are close to their pK. As a result, different conformations of OmpA may coexist depending on side-chain protonation states. This hypothesis is consistent with the observation of coexisting water-soluble states of OmpA near its pI, as evidenced by fluorescence spectroscopy (Qu et al. 2007). Upon dilution of the urea, these forms may engage into different folding pathways. These could either proceed towards the native form at different rates, or one of them could be a dead-end for productive folding so that OmpA would have to unfold again before entering the right pathway. It may be possible that some intramolecular interactions form early after urea dilution and steer OmpA in a productive folding direction, whereas others have to be broken again for folding to the native state. Similar parallel folding pathways as a result of pH-dependent partitioning have been reported for soluble proteins like cytochrome c_{551} (Gianni et al. 2003). A nonproductive intermediate could feature, for instance, interactions between strands that are not nearest neighbors, or hydrogen bonding patterns that are in a wrong sequence, or parallel instead of antiparallel, or that comprise gaps not found in the regular hydrogen bonding pattern between neighboring strands in native OmpA. Likely, intramolecular hydrophobic interactions are different for coexisting forms of OmpA, depending on the protonation state of the lysine and tyrosine side-chains near their pKs. This would be consistent with the fluorescence spectra of OmpA after urea-dilution near its pI (~5.5) and above pH 6.5, which indicate a different hydrophobicity of the environment of the fluorescent tryptophans (Qu et al. 2007). That the balance between pathways may depend on the protonation state of OmpA is strongly suggested by the observation that the relative contributions of the rapid and slow folding processes for OmpA folding into lipid bilayers are pH-dependent (Patel et al. 2009). Since parallel pathways are observed whatever the environment into which OmpA folds, they very likely result from different forms of aqueous OmpA that either are already present in 8 M urea solution or form immediately after urea dilution.

Although the present work does not provide any evidence for intermediate forms, at least one intermediate process must exist, namely the binding of non-natively folded OmpA to A8-35 immediately after urea dilution. The association would be a second-order process, as it would be dependent on the A8-35 concentration. Since this step does not immediately yield the folded state and is not the rate-limiting step, it would not show up in our analysis. Neither the electrophoretic analysis nor the fluorescence measurements can resolve this first stage, because it very likely occurs on a much faster time scale (seconds or faster) than can be detected with the present methods, and would anyway have no signature upon electrophoresis. A collision rate between OmpA and A8-35 particles in the second-to-minute time range can indeed be surmised on the basis of the rate of exchange between protein-bound A8-35 and free particles (Zoonens et al. 2007), taking into account concentration differences between the two sets of experiments.

Once OmpA/A8-35 complexes have formed, the later steps will not depend on the A8-35 concentration, as observed in our study. This is consistent with the two parallel processes being first-order, in contrast to the kinetics of folding of OmpA into large unilamellar vesicles of short-chain phospholipids, which did depend on the concentration of phospholipids (Kleinschmidt and Tamm

2002). It is to be expected that the rate of association of OmpA with A8-35 be much faster than that for association of OmpA with lipid vesicles, which are larger and diffuse more slowly. This view would also be consistent with the observation that, upon folding of OmpA into SUVs of DOPC (Kleinschmidt and Tamm 1996) or dimyristoylphosphatidylcholine (Surrey and Jähnig 1995), fluorescence changes precede the formation of the folded form detected by electrophoresis, in particular at temperatures below 30 °C: because the adsorption of OmpA onto lipid bilayers is slower than its association with A8-35, but faster than folding, it can be kinetically resolved from the latter (Kleinschmidt et al. 2011; Surrey and Jähnig 1995).

Once in contact with A8-35, OmpA folded rapidly. The activation energies for folding into A8-35 were much lower (~5–9 kJ/mol for the fast process and ~29–37 kJ/mol for the slow process) than that reported for DOPC vesicles [46 ± 4 kJ/mol, see ref. Kleinschmidt and Tamm (1996)]. Very likely, A8-35 provides a much more flexible and dynamic environment, which adjusts more rapidly to structural changes in OmpA. We previously pointed out that the flexibility (Marsh et al. 2006) and curvature (Kleinschmidt et al. 2011; Pocanschi et al. 2006c) of the membrane might be a key to faster folding and insertion of OmpA. In *E. coli* cells, such a flexible and dynamic environment is provided by the β-barrel assembly machinery (BAM) complex [see Knowles et al. (2009) for a review].

Stability of OmpA in LDAO and in A8-35

Many previous experiments have shown that TMPs of both the α-helical or the β-barrel types inactivate more slowly, or at higher temperature, once trapped in APols than they do in detergent solutions [see, e.g., Bazzacco et al. (2012); Champeil et al. (2000); Dahmane et al. (2009); Tifrea et al. (2011); Tribet et al. (1996); reviewed by Popot et al. (2011)]. The folding kinetics of bacteriorhodopsin following dilution from an SDS solution has been studied, e.g. Dahmane et al. (2013), but under conditions of irreversibility. The present study is the first one to examine the thermodynamics, in addition to the kinetics, of folding/unfolding of a TMP in APols. Our titrations with urea demonstrate that folding of OmpA is reversible in both LDAO and A8-35. Under our experimental conditions, equilibrium is reached only after more than 20 days of incubation. The data shown in Fig. 6 indicate that it is the unfolding reaction that requires these long incubation times. After a sufficiently long incubation, the unfolding titration curves of both OmpA in A8-35 and OmpA in LDAO superimpose to the folding titration curves observed after the shortest investigated incubation times (3 days). This suggests that the activation energy for OmpA unfolding is very large, in particular in the presence of A8-35, for which 52 days of incubation were necessary until unfolding titration curves superimposed onto the folding ones. For LDAO, the necessary incubation time was only half as long. This is consistent with the protecting nature of A8-35 observed in previous, kinetic denaturation experiments. It seems also to tally with the suggestion that the free energy cost of reorganizing the backbone of the polymer around the transmembrane surface of TMPs damps conformational rearrangements that affect this surface, which has been proposed to contribute to slowing down denaturation kinetics (Picard et al. 2006; Popot et al. 2003, 2011).

For folding titration curves, as well as after the longest incubation times for unfolding ones—that is, when both curves superimpose, midpoints are observed at 6 M urea in LDAO and 2 M urea in A8-35. It is interesting to compare this with a previous study (Pocanschi et al. 2006c), where folding/unfolding of OmpA was monitored using large unilamellar vesicles of either *di*C_{12}PC or *di*C_{12}PC/*di*C_{12}PG at a 1:1 molar ratio. In these lipid systems, an unfolding titration could not be observed even after 12 days of incubation, whereas the folding titration had a midpoint around 2 M urea, similar to that observed here for folding into A8-35. In lipid vesicles, the activation energy for unfolding was very high and prevented the estimation of the free energy from unfolding titrations.

In comparison to folding into LDAO, OmpA therefore folds at lower concentrations of urea either in A8-35 or lipid vesicles. The transitions are also steeper in LDAO than in A8-35 or in lipid bilayers (Pocanschi et al. 2006c), which suggests a higher cooperativity of folding in LDAO. Since the free energy gain of folding, which corresponds to the free energy necessary for unfolding, is larger in LDAO than in A8-35, the folded form of OmpA appears to be thermodynamically more stable in LDAO than in A8-35. As a result, at least at pH 10, OmpA is more resistant to unfolding by urea in the neutral detergent LDAO than in negatively charged A8-35. It may be that the destabilization in A8-35 is a consequence of the deprotonation of some of the 17 lysine side-chains (pK ~ 9.5–10.5) of OmpA (pI ~ 5.5) or some of its 17 tyrosine side-chains (pK ~ 9.5–10). At pH 10, OmpA is highly negatively charged and interactions with negatively charged A8-35 might destabilize OmpA/A8-35 complexes. Charge-charge repulsion indeed has been reported previously to destabilize OmpA and to slow down its folding in lipid bilayers (Surrey and Jähnig 1995). It will be of interest to examine the stability of OmpA in non-ionic APols (Bazzacco et al. 2012; Sharma et al. 2012), where electrostatic repulsion between the protein and the APol will be inexistent even at high pH.

The dependence of the apparent free energy of stabilization on urea concentration is linear in the titration region

where folded and unfolded forms coexist, as reported previously for OmpA in lipid bilayers (Hong and Tamm 2004). However, folded and unfolded forms are in true equilibrium only where the titration curves of folding and unfolding superimpose, that is after sufficiently long incubation times. Free energies at 0 M urea are typically obtained by fitting Eq. 6 to the titration curves, which includes a linear extrapolation of the free energy to 0 M urea. Since the presence of a surfactant is necessary for equilibrium unfolding studies of membrane proteins, it cannot be entirely excluded that the higher thermodynamic stability of OmpA seen in LDAO [or in octylmaltoside (Andersen et al. 2012)] versus A8-35 be due to surfactant-urea interactions.

Recent circular dichroism studies have shown that, at pH 7.3, the major outer membrane protein from *Chlamydia trachomatis*, MOMP, a β-barrel trimer (pI $\approx$ 4.4), is strongly stabilized against thermal denaturation (by >30 °C) when trapped in A8-35 rather than solubilized in zwittergent 3–14 (Tifrea et al. 2011). Heat denaturation is not reversible, because the denatured protein aggregates and precipitates. Furthermore, it is typically performed at heating rates faster than is necessary for equilibration. A Gibbs free energy for folding/unfolding can therefore not be obtained in this way. It is not known, therefore, whether the stabilization of MOMP by A8-35 is of kinetic or of thermodynamic origin.

Conclusion

In summary, the present data show that OmpA efficiently folds and its rate of denaturation by urea is strongly slowed down in APol A8-35 as compared to the detergent LDAO. Protection against urea-induced denaturation is not due to a higher thermodynamic stability of the folded state in A8-35, but to a higher kinetic barrier to unfolding. The lower thermodynamic stability of OmpA in A8-35 versus LDAO may result from the high pH used in the experiments, which creates electrostatic repulsion between the protein and the APol, both of which are negatively charged under these conditions.

Acknowledgments Particular thanks are due to Fabrice Giusti (CNRS UMR 7099, Paris) for synthesizing the batches of A8-35 used in the present work, as well as for information about the revised estimate of its average molecular mass. This work was supported by grants KL 1024/2-5 and 2-6 from the Deutsche Forschungsgemeinschaft to J.H.K.

References

Althoff T, Mills DJ, Popot JL, Kühlbrandt W (2011) Arrangement of electron transport chain components in bovine mitochondrial supercomplex $I_1III_2IV_1$. EMBO J 30:4652–4664

Andersen KK, Wang H, Otzen DE (2012) A kinetic analysis of the folding and unfolding of OmpA in urea and guanidinium chloride: single and parallel pathways. Biochemistry 51:8371–8383

Arora A, Rinehart D, Szabo G, Tamm LK (2000) Refolded outer membrane protein A of *Escherichia coli* forms ion channels with two conductance states in planar lipid bilayers. J Biol Chem 275:1594–1600

Banères JL, Popot JL, Mouillac B (2011) New advances in production and functional folding of G-protein-coupled receptors. Trends Biotechnol 29:314–322

Bazzacco P, Billon-Denis E, Sharma KS, Catoire LJ, Mary S, Le Bon C, Point E, Banères JL, Durand G, Zito F, Pucci B, Popot JL (2012) Nonionic homopolymeric amphipols: application to membrane protein folding, cell-free synthesis, and solution nuclear magnetic resonance. Biochemistry 51:1416–1430

Buchanan SK (1999) β-barrel proteins from bacterial outer membranes: structure, function and refolding. Curr Opin Struct Biol 9:455–461

Bulieris PV, Behrens S, Holst O, Kleinschmidt JH (2003) Folding and insertion of the outer membrane protein OmpA is assisted by the chaperone Skp and by lipopolysaccharide. J Biol Chem 278:9092–9099

Catoire LJ, Zoonens M, van Heijenoort C, Giusti F, Popot JL, Guittet E (2009) Inter- and intramolecular contacts in a membrane protein/surfactant complex observed by heteronuclear dipole-to-dipole cross-relaxation. J Magn Reson 197:91–95

Catoire LJ, Zoonens M, van Heijenoort C, Giusti F, Guittet E, Popot JL (2010) Solution NMR mapping of water-accessible residues in the transmembrane β-barrel of OmpX. Eur Biophys J 39:623–630

Champeil P, Menguy T, Tribet C, Popot JL, le Maire M (2000) Interaction of amphipols with sarcoplasmic reticulum Ca^{2+}-ATPase. J Biol Chem 275:18623–18637

Dahmane T, Damian M, Mary S, Popot JL, Banères JL (2009) Amphipol-assisted in vitro folding of G protein-coupled receptors. Biochemistry 48:6516–6521

Dahmane T, Giusti F, Catoire LJ, Popot JL (2011) Sulfonated amphipols: synthesis, properties, and applications. Biopolymers 95:811–823

Dahmane T, Rappaport F, Popot JL (2013) Amphipol-assisted folding of bacteriorhodopsin in the presence or absence of lipids: functional consequences. Eur Biophys J. doi:10.1007/s00249-012-0839-z

Dornmair K, Kiefer H, Jähnig F (1990) Refolding of an integral membrane protein. OmpA of *Escherichia coli*. J Biol Chem 265:18907–18911

Gianni S, Travaglini-Allocatelli C, Cutruzzola F, Brunori M, Shastry MC, Roder H (2003) Parallel pathways in cytochrome c_{551} folding. J Mol Biol 330:1145–1152

Giusti F, Popot JL, Tribet C (2012) Well-defined critical association concentration and rapid adsorption at the air/water interface of a short amphiphilic polymer, amphipol A8-35: a study by Förster resonance energy transfer and dynamic surface tension measurements. Langmuir 28:10372–10380

Gohon Y, Pavlov G, Timmins P, Tribet C, Popot J-L, Ebel C (2004) Partial specific volume and solvent interactions of amphipol A8-35. Anal Biochem 334:318–334

Gohon Y, Giusti F, Prata C, Charvolin D, Timmins P, Ebel C, Tribet C, Popot JL (2006) Well-defined nanoparticles formed by hydrophobic assembly of a short and polydisperse random terpolymer, amphipol A8-35. Langmuir 22:1281–1290

He S, Wang B, Chen H, Tang C, Feng Y (2012) Preparation and antimicrobial properties of gemini surfactant-supported triiodide complex system. ACS Appl Mater Interfaces 4:2116–2123

Hong H, Tamm LK (2004) Elastic coupling of integral membrane protein stability to lipid bilayer forces. Proc Natl Acad Sci USA 101:4065–4070

Kiefer H (2003) In vitro folding of α-helical membrane proteins. Biochim Biophys Acta 1610:57–62

Kleinschmidt JH (2003) Membrane protein folding on the example of outer membrane protein A of *Escherichia coli*. Cell Mol Life Sci 60:1547–1558

Kleinschmidt JH (2006) Folding kinetics of the outer membrane proteins OmpA and FomA into phospholipid bilayers. Chem Phys Lipids 141:30–47

Kleinschmidt JH, Tamm LK (1996) Folding intermediates of a β-barrel membrane protein. Kinetic evidence for a multi-step membrane insertion mechanism. Biochemistry 35:12993–13000

Kleinschmidt JH, Tamm LK (1999) Time-resolved distance determination by tryptophan fluorescence quenching: probing intermediates in membrane protein folding. Biochemistry 38:4996–5005

Kleinschmidt JH, Tamm LK (2002) Secondary and tertiary structure formation of the β-barrel membrane protein OmpA is synchronized and depends on membrane thickness. J Mol Biol 324:319–330

Kleinschmidt JH, den Blaauwen T, Driessen A, Tamm LK (1999a) Outer membrane protein A of *E. coli* inserts and folds into lipid bilayers by a concerted mechanism. Biochemistry 38:5006–5016

Kleinschmidt JH, Wiener MC, Tamm LK (1999b) Outer membrane protein A of *E. coli* folds into detergent micelles, but not in the presence of monomeric detergent. Protein Sci 8:2065–2071

Kleinschmidt JH, Bulieris PV, Qu J, Dogterom M, den Blaauwen T (2011) Association of neighboring β–strands of outer membrane protein A in lipid bilayers revealed by site directed fluorescence quenching. J Mol Biol 407:316–332

Knowles TJ, Scott-Tucker A, Overduin M, Henderson IR (2009) Membrane protein architects: the role of the BAM complex in outer membrane protein assembly. Nat Rev Microbiol 7:206–214

Laemmli UK (1970) Cleavage of structural proteins during the assembly of the head of bacteriophage T4. Nature 227:680–685

Leney AC, McMorran LM, Radford SE, Ashcroft AE (2012) Amphipathic polymers enable the study of functional membrane proteins in the gas phase. Anal Chem 84:9841–9847

Lowry OH, Rosebrough NJ, Farr AL, Randall RJ (1951) Protein measurement with the Folin phenol reagent. J Biol Chem 193:265–275

Marsh D, Shanmugavadivu B, Kleinschmidt JH (2006) Membrane elastic fluctuations and the insertion and tilt of β-barrel proteins. Biophys J 91:227–232

Pace CN (1990) Measuring and increasing protein stability. Trends Biotechnol 8:93–98

Pace CN, Shaw KL (2000) Linear extrapolation method of analyzing solvent denaturation curves. Proteins Suppl 4:1–7

Pace CN, Hebert EJ, Shaw KL, Schell D, Both V, Krajcikova D, Sevcik J, Wilson KS, Dauter Z, Hartley RW, Grimsley GR (1998) Conformational stability and thermodynamics of folding of ribonucleases Sa, Sa2 and Sa3. J Mol Biol 279:271–286

Patel GJ, Behrens-Kneip S, Holst O, Kleinschmidt JH (2009) The periplasmic chaperone Skp facilitates targeting, insertion and folding of OmpA into lipid membranes with a negative membrane surface potential. Biochemistry 48:10235–10245

Pautsch A, Schulz GE (1998) Structure of the outer membrane protein A transmembrane domain. Nat Struct Biol 5:1013–1017

Perlmutter JD, Drasler WJ 2nd, Xie W, Gao J, Popot JL, Sachs JN (2011) All-atom and coarse-grained molecular dynamics simulations of a membrane protein stabilizing polymer. Langmuir 27:10523–10537

Picard M, Dahmane T, Garrigos M, Gauron C, Giusti F, le Maire M, Popot JL, Champeil P (2006) Protective and inhibitory effects of various types of amphipols on the Ca^{2+}-ATPase from sarcoplasmic reticulum: a comparative study. Biochemistry 45:1861–1869

Pocanschi CL, Apell H-J, Puntervoll P, Høgh BT, Jensen HB, Welte W, Kleinschmidt JH (2006a) The major outer membrane protein of *Fusobacterium nucleatum* (FomA) folds and inserts into lipid bilayers via parallel folding pathways. J Mol Biol 355:548–561

Pocanschi CL, Dahmane T, Gohon Y, Rappaport F, Apell H-J, Kleinschmidt JH, Popot J-L (2006b) Amphipathic polymers: tools to fold integral membrane proteins to their active form. Biochemistry 45:13954–13961

Pocanschi CL, Patel GJ, Marsh D, Kleinschmidt JH (2006c) Curvature elasticity and refolding of OmpA in large unilamellar vesicles. Biophys J 91:L75–L78

Popot JL (2010) Amphipols, nanodiscs, and fluorinated surfactants: three nonconventional approaches to studying membrane proteins in aqueous solutions. Annu Rev Biochem 79:737–775

Popot JL, Engelman DM (2000) Helical membrane protein folding, stability, and evolution. Annu Rev Biochem 69:881–922

Popot JL, Berry EA, Charvolin D, Creuzenet C, Ebel C, Engelman DM, Flötenmeyer M, Giusti F, Gohon Y, Hong Q, Lakey JH, Leonard K, Shuman HA, Timmins P, Warschawski DE, Zito F, Zoonens M, Pucci B, Tribet C (2003) Amphipols: polymeric surfactants for membrane biology research. Cell Mol Life Sci 60:1559–1574

Popot JL, Althoff T, Bagnard D, Banerès JL, Bazzacco P, Billon-Denis E, Catoire LJ, Champeil P, Charvolin D, Cocco MJ, Cremel G, Dahmane T, de la Maza LM, Ebel C, Gabel F, Giusti F, Gohon Y, Goormaghtigh E, Guittet E, Kleinschmidt JH, Kühlbrandt W, Le Bon C, Martinez KL, Picard M, Pucci B, Sachs JN, Tribet C, van Heijenoort C, Wien F, Zito F, Zoonens M (2011) Amphipols from A to Z. Annu Rev Biophys 40:379–408

Qu J, Mayer C, Behrens S, Holst O, Kleinschmidt JH (2007) The trimeric periplasmic chaperone Skp of *Escherichia coli* forms 1:1 complexes with outer membrane proteins via hydrophobic and electrostatic interactions. J Mol Biol 374:91–105

Rodionova NA, Tatulian SA, Surrey T, Jähnig F, Tamm LK (1995) Characterization of two membrane-bound forms of OmpA. Biochemistry 34:1921–1929

Roumestand C, Boyer M, Guignard L, Barthe P, Royer CA (2001) Characterization of the folding and unfolding reactions of a small β-barrel protein of novel topology, the MTCP1 oncogene product P13. J Mol Biol 312:247–259

Royer CA, Mann CJ, Matthews CR (1993) Resolution of the fluorescence equilibrium unfolding profile of trp aporepressor using single tryptophan mutants. Protein Sci 2:1844–1852

Sanders CR, Kuhn Hoffmann A, Gray DN, Keyes MH, Ellis CD (2004) French swimwear for membrane proteins. Chembiochem 5:423–426

Schweizer M, Hindennach I, Garten W, Henning U (1978) Major proteins of the *Escherichia coli* outer cell envelope membrane. Interaction of protein II with lipopolysaccharide. Eur J Biochem 82:211–217

Sharma KS, Durand G, Gabel F, Bazzacco P, Le Bon C, Billon-Denis E, Catoire LJ, Popot JL, Ebel C, Pucci B (2012) Non-ionic amphiphilic homopolymers: synthesis, solution properties, and biochemical validation. Langmuir 28:4625–4639

Sugawara E, Steiert M, Rouhani S, Nikaido H (1996) Secondary structure of the outer membrane proteins OmpA of *Escherichia coli* and OprF of *Pseudomonas aeruginosa*. J Bacteriol 178:6067–6069

Surrey T, Jähnig F (1992) Refolding and oriented insertion of a membrane protein into a lipid bilayer. Proc Natl Acad Sci USA 89:7457–7461

Surrey T, Jähnig F (1995) Kinetics of folding and membrane insertion of a β-barrel membrane protein. J Biol Chem 270:28199–28203

Tifrea DF, Sun G, Pal S, Zardeneta G, Cocco MJ, Popot JL, de la Maza LM (2011) Amphipols stabilize the *Chlamydia* major outer

membrane protein and enhance its protective ability as a vaccine. Vaccine 29:4623–4631

Tribet C, Audebert R, Popot JL (1996) Amphipols: polymers that keep membrane proteins soluble in aqueous solutions. Proc Natl Acad Sci USA 93:15047–15050

van Holde KE, Curtis Johnson W, Shing Ho P (2006) Principles of physical biochemistry, 2nd edn. Pearson Prentice Hall, London

Vogel H, Jähnig F (1986) Models for the structure of outer-membrane proteins of *Escherichia coli* derived from Raman spectroscopy and prediction methods. J Mol Biol 190:191–199

Walser R, Kleinschmidt JH, Zerbe O (2011) A chimeric GPCR model mimicking the ligand binding site of the human Y1 receptor studied by NMR spectroscopy. Chembiochem 12:1690–1693

Walser R, Kleinschmidt JH, Skerra A, Zerbe O (2012) β-Barrel scaffolds for the grafting of extracellular loops from G protein-coupled receptors. Biol Chem 393:1341–1355

Weber K, Osborne M (1964) The reliability of molecular weight determinations by dodecyl sulfate-polyacrylamide gel electrophoresis. J Biol Chem 244:4406–4412

Zoonens M, Giusti F, Zito F, Popot JL (2007) Dynamics of membrane protein/amphipol association studied by Förster resonance energy transfer: implications for in vitro studies of amphipol-stabilized membrane proteins. Biochemistry 46:10392–10404